Flexible Joints - Test Bench

Dehaeze Thomas

April 5, 2024

Contents

At both ends of the nano-hexapod struts, a flexible spherical joint is used. Ideally, these flexible joints would behave as perfect spherical joints, that is to say no bending and torsional stiffnesses, infinite shear and axial stiffnesses, unlimited bending and torsional stroke, no friction and no backlash.

Deviations from this ideal properties will impact the dynamics of the Nano-Hexapod and could limit the attainable performances. During the detailed design phase, specifications in term of stiffness and stroke have been determined and are summarized in Table 1.

	Specification	**FEM**
Axial Stiffness	$> 100\,N/\mu m$	94
Shear Stiffness	$> 1\,N/\mu m$	13
Bending Stiffness	$< 100\,Nm/\text{rad}$	5
Torsion Stiffness	$< 500\,Nm/\text{rad}$	260
Bending Stroke	$> 1\,\text{mrad}$	24.5

Table 1: Specifications for the flexible joints and estimated characteristics from the Finite Element Model

After optimization using a finite element model, the geometry shown in Figure 1 has been obtained and the corresponding flexible joints characteristics are summarized in Table 1. This flexible joint is a monolithic piece of stainless steel[1] manufactured using wire electrical discharge machining. It serves several functions as shown in Figure 1a, such as:

- Rigid interfacing with the nano-hexapod plates (yellow surfaces)
- Rigid interfacing with the amplified piezoelectric actuator (blue surface)
- Allow two rotations between the "yellow" and the "blue" interfaces. The rotation axes are represented by the dashed lines which are intersecting

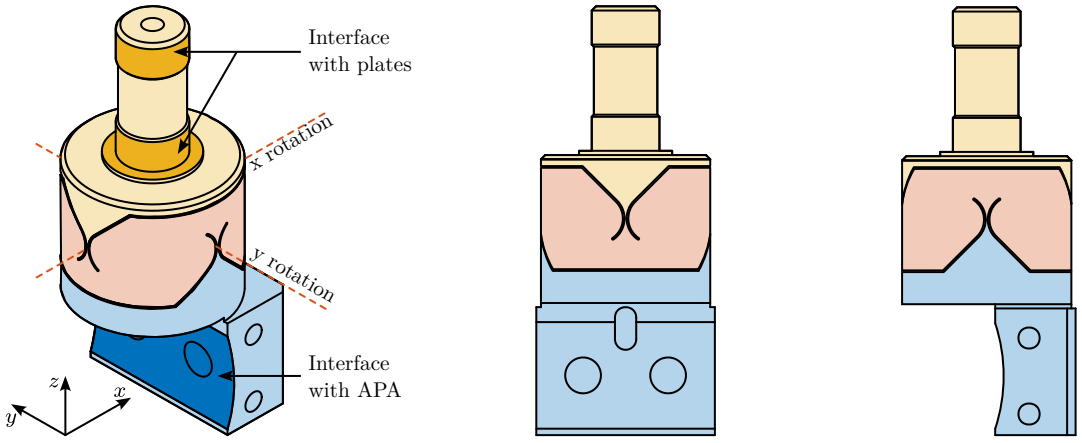

(a) ISO view **(b)** YZ plane **(c)** XZ plane

Figure 1: Geometry of the optimized flexible joints

16 flexible joints have been ordered (shown in Figure 2a) such some selection can be made for the 12 that will be used on the nano-hexapod.

[1]The alloy used is called *F16PH*, also refereed as "1.4542"

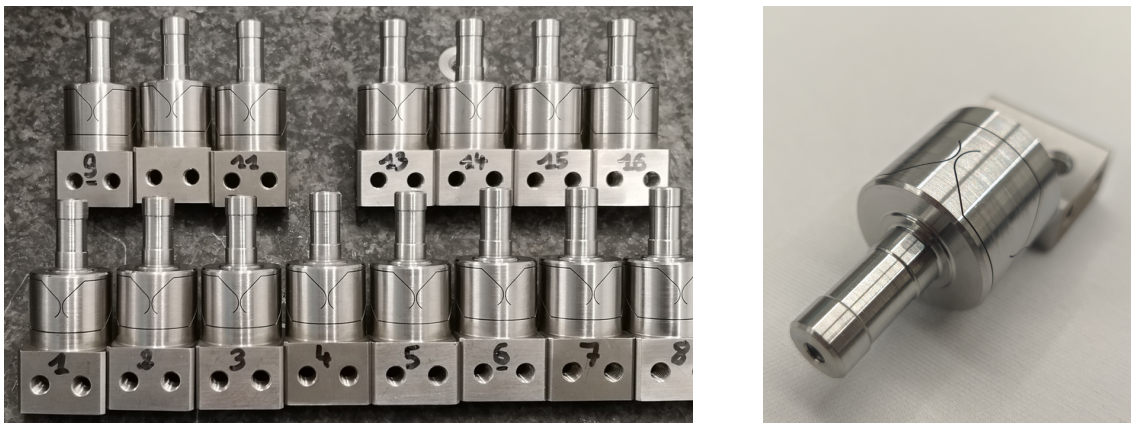

(a) 15 of the 16 received flexible joints

(b) Zoom on one flexible joint

Figure 2: Pictures of the received 16 flexible joints

In this document, the received flexible joints are characterize to make sure they are fulfilling the requirements and such that they can well be modelled.

First, the flexible joints are visually inspected, and the minimum gaps (responsible for most of the joint compliance) are measured (Section 1). Then, a test bench is developed to measure the bending stiffness of the flexible joints. The development of this test bench is presented in Section 2, including a noise budget and some requirements in terms of instrumentation. Finally, the test bench is manufacturer and used to measure the bending stiffnesses of all the flexible joints. Results are shown in Section 3

Sections	**Matlab File**
Section 1	`test_joints_1_dim_meas.m`
Section 2	`test_joints_2_bench_dimensioning.m`
Section 3	`test_joints_3_bending_stiff_meas.m`

Table 2: Report sections and corresponding Matlab files

1 Dimensional Measurements

1.1 Measurement Bench

The dimensions of the flexible part in the Y-Z plane will contribute to the X-bending stiffness. Similarly, the dimensions of the flexible part in the X-Z plane will contribute to the Y-bending stiffness.

The setup to measure the dimension of the "X" flexible beam is shown in Figure 1.1b.

What we typically observe is shown in Figure 1.1a. It is then possible to estimate to dimension of the flexible beam with an accuracy of $\approx 5\,\mu m$,

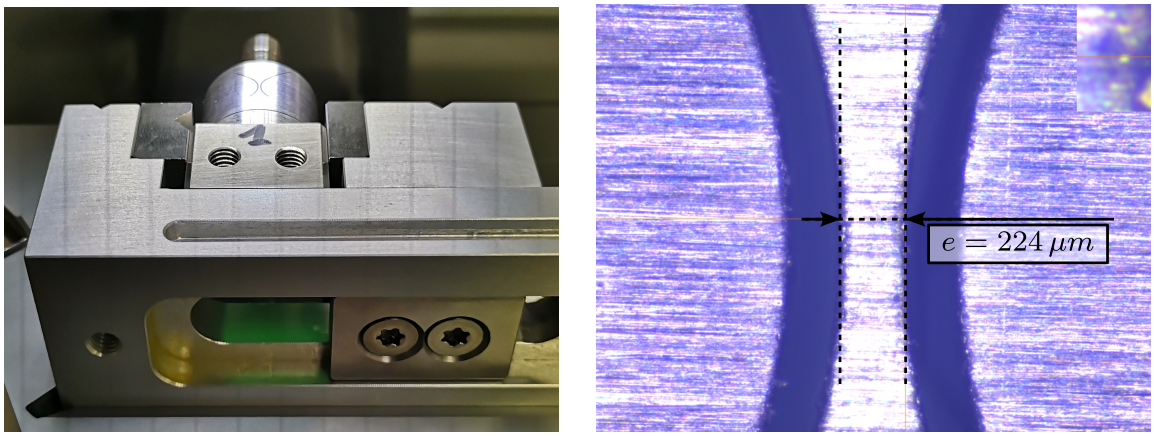

(a) Flexible joint fixed on the profilometer

(b) Obtain image to estimate the gap

Figure 1.1: Setup to measure the dimension of the flexible beam corresponding to the X-bending stiffness. The flexible joint is fixed to the profilometer (a) and a image is obtained with which the gap can be estimated (b)

1.2 Measurement Results

The specified flexible beam thickness (gap) is $250\,\mu m$. Four gaps are measured for each flexible joints (2 in the x direction and 2 in the y direction). The "beam thickness" is then estimated to be the mean between the gaps measured on opposite sides.

An histogram of the measured beam thicknesses is shown in Figure 1.2. The measured thickness is less thant the specified value of $250\,\mu m$, but this optical method may not be very accurate as the estimated gap can depend on the lighting of the part and of its proper alignment.

However, what is more important than the true value of the thickness is the consistency between all the flexible joints.

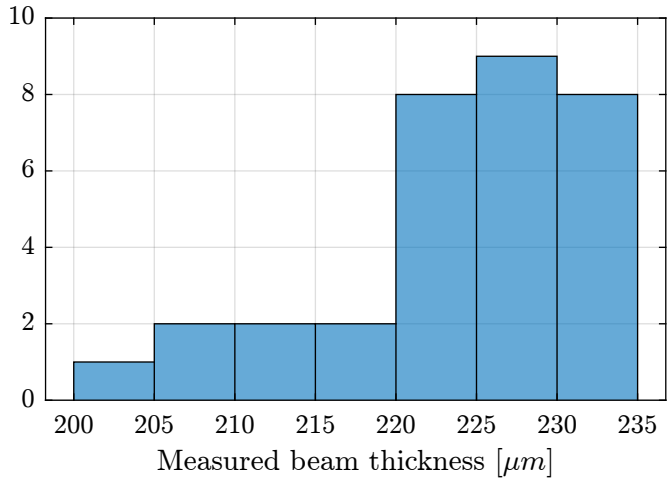

Figure 1.2: Histogram for the (16x2) measured beams' thickness

1.3 Bad flexible joints

Using this profilometer allowed to detect flexible joints with manufacturing defects such as non-symmetrical shape (see Figure 1.3a) or flexible joints with machining chips stuck in the gap (see Figure 1.3b).

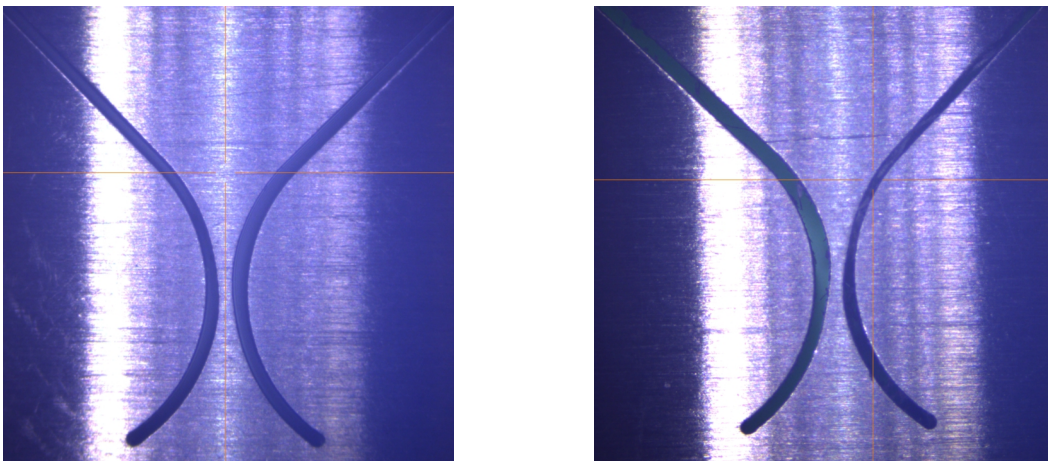

(a) Non-Symmetrical shape

(b) "Chips" stuck in the air gap

Figure 1.3: Example of two flexible joints that were considered unsatisfactory after visual inspection

2 Development of the Measurement Test Bench

The most important characteristic of the flexible joint to be measured is its bending stiffness $k_{R_x} \approx k_{R_y}$.

To estimate the bending stiffness, the basic idea is to apply a torque T_x to the flexible joints and to measure its angular deflection θ_x. Then, the bending stiffness can be computed from equation (2.1).

$$\boxed{k_{R_x} = \frac{T_x}{\theta_x}, \quad k_{R_y} = \frac{T_y}{\theta_y}} \tag{2.1}$$

2.1 Measurement principle

Torque and Rotation measurement In order to apply torque T_y between the two mobile parts of the flexible joint, a known "linear" force F_x can be applied instead at the certain height h with respect to the rotation point. In that case the equivalent applied torque can be estimated from equation (2.2). Note that the application point of the force should be far enough from the rotation axis such that the resulting bending motion is much larger than the displacement due to shear. Such effect is studied in Section 2.3.

$$T_y = hF_x, \quad T_x = hF_y \tag{2.2}$$

Similarly, instead of directly measuring the bending motion θ_y of the flexible joint, its linear motion d_x at a certain height h from the rotation points is measured. The equivalent rotation is estimated from (2.3).

$$\theta_y = \tan^{-1}\left(\frac{d_x}{h}\right) \approx \frac{d_x}{h}, \quad \theta_x = \tan^{-1}\left(\frac{d_y}{h}\right) \approx \frac{d_y}{h} \tag{2.3}$$

Then, the bending stiffness can be estimated from (2.4).

$$k_{R_x} = \frac{T_x}{\theta_x} = \frac{hF_y}{\tan^{-1}\left(\frac{d_y}{h}\right)} \approx h^2\frac{F_y}{d_y} \tag{2.4a}$$

$$k_{R_y} = \frac{T_y}{\theta_y} = \frac{hF_x}{\tan^{-1}\left(\frac{d_x}{h}\right)} \approx h^2\frac{F_x}{d_x} \tag{2.4b}$$

The working principle of the measurement bench is schematically shown in Figure 2.1. One part of the flexible joint is fixed to a rigid frame while a (known) force F_x is applied to the other side of the flexible joint. The deflection of the joint d_x is measured by a displacement sensor.

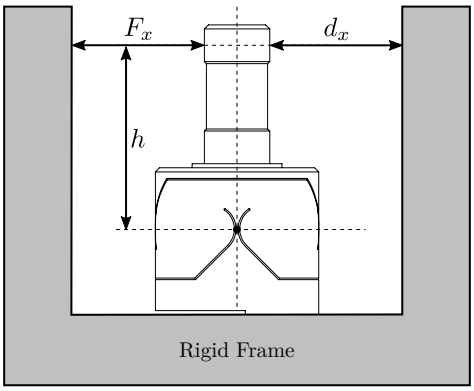

Figure 2.1: Workind principle of the test bench used to estimate the bending stiffness k_{R_y} of the flexible joints by measuring F_x, d_x and h

Required external applied force The bending stiffness is foreseen to be $k_{R_y} \approx k_{R_x} \approx 5\,\frac{Nm}{rad}$ and its stroke $\theta_{y,\max} \approx \theta_{x,\max} \approx 25\,mrad$. The height between the flexible point (center of the joint) and the point where external forces are applied is $h = 22.5\,mm$ (see Figure 2.1).

The bending θ_y of the flexible joint due to the force F_x is given by equation (2.5).

$$\theta_y = \frac{T_y}{k_{R_y}} = \frac{F_x h}{k_{R_y}} \tag{2.5}$$

Therefore, the force that has to be applied to test the full range of the flexible joint is given by equation (2.6). The measurement range of the force sensor should then be higher than $5.5\,N$.

$$F_{x,\max} = \frac{k_{R_y}\theta_{y,\max}}{h} \approx 5.5\,N \tag{2.6}$$

Required actuator stroke and sensors range The flexible joint is designed to allow a bending motion of $\pm 25\,mrad$. The corresponding stroke at the location of the force sensor is given by (2.7). In order to test the full range of the flexible joint, the means of applying a force (explained in the next section) should allow a motion of at least $0.5\,mm$. Similarly, the measurement range of the displacement sensor should also be higher than $0.5\,mm$.

$$d_{x,\max} = h\tan(R_{x,\max}) \approx 0.5\,mm \tag{2.7}$$

2.2 Developed test bench

As explained in Section 2.1, the flexible joint's bending stiffness is estimated by applying a known force to the flexible joint's tip and by measuring its deflection at the same point.

The force is applied using a load cell[1] such that the applied force to the flexible joint's tip is directly measured. In order to control the height and direction of the applied force, a cylinder cut in half is fixed at the tip of the force sensor (pink element in Figure 2.2b) that initially had a flat surface. This way, the contact between the flexible joint cylindrical tip and the force sensor is a point (intersection of two cylinders) at a precise height, and the force is applied in a known direction. To translate the load cell at a constant height, it is fixed to a translation stage[2] which is moved by hand.

Instead of measuring the displacement directly at the tip of the flexible joint (with a probe or an interferometer for instance), the displacement of the load cell itself is measured. To do so, an encoder[3] is used that measures the motion of a ruler. This ruler is fixed to the translation stage in line (i.e. at the same height) with the application point to reduce Abbe errors (see Figure 2.2a). Indirectly measuring the deflection of the flexible joint induces some errors due to the limited stiffness between the tip of the force sensor and the ruler. Such error will be estimated in Section 2.3.

The flexible joint can be rotated by 90 degrees in order to measure the bending stiffness in the two directions. The obtained CAD design of the measurement bench is shown in Figure 2.2a while a zoom on the flexible joint with the associated important quantities is shown in Figure 2.2b.

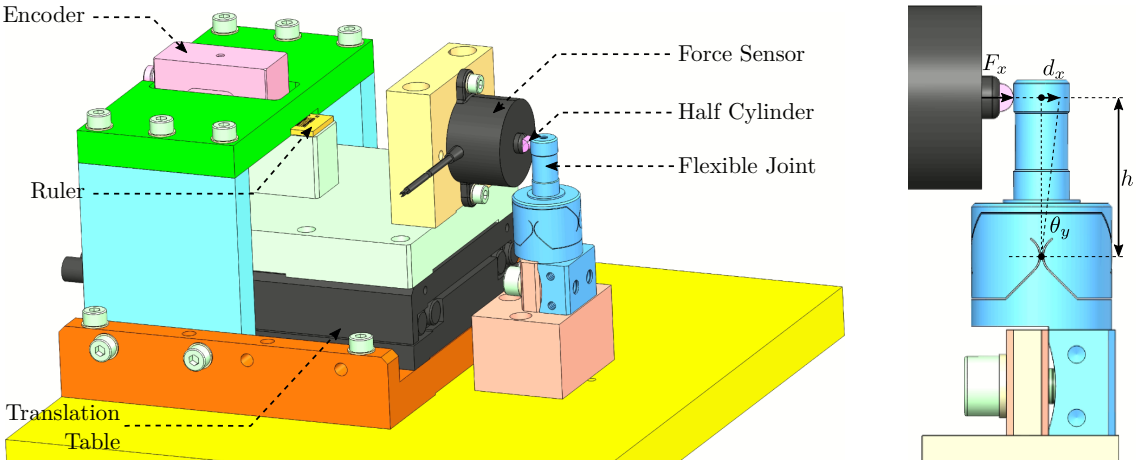

(a) Schematic of the test bench to measure the bending stiffness of the flexible joints **(b)** Zoom

Figure 2.2: CAD view of the test bench developped to measure the bending stiffness of the flexible joints. Different parts are shown in (a) while a zoom on the flexible joint is shown in (b)

[1] The load cell is FC22 from TE Connectivity. Measurement range is $50\,N$. Specified accuracy is 1 % of the full range
[2] V-408 PIMag® linear stage is used. Crossed roller are used to guide the motion.
[3] Resolute™ encoder with $1\,nm$ resolution and $\pm 40\,nm$ maximum non-linearity

2.3 Error budget

In order to estimate the accuracy of the measured bending stiffness that can be obtained using this measurement bench, an error budget is performed.

Based on equation (2.4), several errors can impact the accuracy of the measured bending stiffness:

- Errors in the measured torque M_x, M_y: this is mainly due to inaccuracies of the load cell and of the height estimation h
- Errors in the measured bending motion of the flexible joints θ_x, θ_y: errors from limited shear stiffness, from the deflection of the load cell itself, and from inaccuracy of the height estimation h

Let's first estimate the displacement induced only by the bending stiffness.

$$d_{x,b} = h \tan(\theta_y) = h \tan\left(\frac{F_x \cdot h}{k_{R_y}}\right) \tag{2.8}$$

Effect of Shear The applied force F_x will induce some shear $d_{x,s}$ which is described by (2.9) with k_s the shear stiffness of the flexible joint.

$$d_{x,s} = \frac{F_x}{k_s} \tag{2.9}$$

The measured displacement d_x is affected by the shear as shown in equation (2.10).

$$d_x = d_{x,b} + d_{x,s} = h \tan\left(\frac{F_x \cdot h}{k_{R_y}}\right) + \frac{F_x}{k_s} \approx F_x \left(\frac{h^2}{k_{R_y}} + \frac{1}{k_s}\right) \tag{2.10}$$

The estimated bending stiffness k_{est} then depends on the shear stiffness (2.11).

$$k_{R_y,\text{est}} = h^2 \frac{F_x}{d_x} \approx k_{R_y} \frac{1}{1 + \frac{k_{R_y}}{k_s h^2}} \approx k_{R_y} \Big(1 - \underbrace{\frac{k_{R_y}}{k_s h^2}}_{\epsilon_s}\Big) \tag{2.11}$$

With an estimated shear stiffness $k_s = 13\, N/\mu m$ from the finite element model and an height $h = 25\, mm$, the estimation errors of the bending stiffness due to shear is $\epsilon_s < 0.1\,\%$

Effect of load cell limited stiffness As explained in the previous section, because the measurement of the flexible joint deflection is indirectly made with the encoder, errors will be made if the load cell experiences some compression.

Suppose the load cell has an internal stiffness k_f, the same reasoning that was made for the effect of shear can be applied here. The estimation error of the bending stiffness due to the limited stiffness of the load cell is then described by (2.12).

$$k_{R_y,\text{est}} = h^2 \frac{F_x}{d_x} \approx k_{R_y} \frac{1}{1 + \frac{k_{R_y}}{k_F h^2}} \approx k_{R_y} \Big(1 - \underbrace{\frac{k_{R_y}}{k_F h^2}}_{\epsilon_f}\Big) \tag{2.12}$$

With an estimated load cell stiffness of $k_f \approx 1\, N/\mu m$ (from the documentation), the errors due to the load cell limited stiffness is around $\epsilon_f = 1\,\%$.

Estimation error due to height estimation error Let's consider an error δh in the estimation of the height h as described by (2.13).

$$h_{\text{est}} = h + \delta h \tag{2.13}$$

The computed bending stiffness will be (2.14).

$$k_{R_y,\text{est}} \approx h_{\text{est}}^2 \frac{F_x}{d_x} \approx k_{R_y} \Big(1 + \underbrace{2\frac{\delta h}{h} + \frac{\delta h^2}{h^2}}_{\epsilon_h}\Big) \tag{2.14}$$

The height estimation is foreseen to be accurate to within $|\delta h| < 0.4\, mm$ which corresponds to a stiffness error $\epsilon_h < 3.5\,\%$.

Estimation error due to force and displacement sensors accuracy The maximum error of the measured displacement due the encoder non-linearity is $40\, nm$. As the measured displacement is foreseen to be $0.5\, mm$, the error ϵ_d due to the encoder non linearity is very small $\epsilon_d < 0.01\,\%$.

The accuracy of the load cell is specified at $1\,\%$ and therefore, estimation errors of the bending stiffness due to the limited load cell accuracy should be $\epsilon_F < 1\,\%$

Conclusion The different sources of errors are summarized in Table 2.1. The most important source of error comes from estimation error of the distance between the flexible joint rotation axis and its contact with the force sensor. An overall accuracy of $\approx 5\,\%$ can be expected with this measurement bench, which should be enough for a first estimation of the bending stiffness of the flexible joints.

Effect	**Error**
Shear effect	$\epsilon_s < 0.1\,\%$
Load cell compliance	$\epsilon_f = 1\,\%$
Height error	$\epsilon_h < 3.5\,\%$
Displacement sensor	$\epsilon_d < 0.01\,\%$
Force sensor	$\epsilon_F < 1\,\%$

Table 2.1: Summary of the error budget for the estimation of the bending stiffness

3 Bending Stiffness Measurement

3.1 Introduction

A picture of the bench used to measure the X-bending stiffness of the flexible joints is shown in Figure 3.1a. A closer view on the force sensor tip is shown in Figure 3.1b.

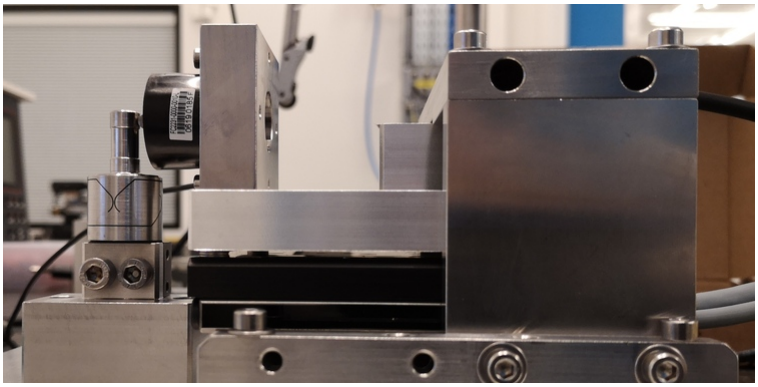

(a) Picture of the measurement bench

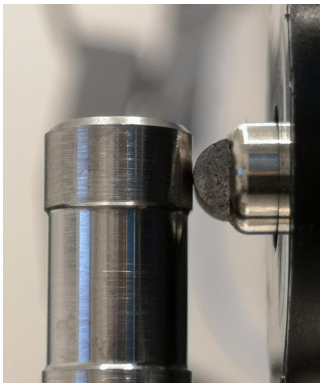

(b) Zoom on the tip

Figure 3.1: Caption with reference to sub figure (**??**)

3.2 Load Cell Calibration

In order to estimate the measured errors of the load cell "FC2231", it is compared against another load cell[1]. The two load cells are measured simultaneously while they are pushed against each other (see Figure 3.2a). The contact between the two load cells is well defined as one has a spherical interface while the other has a flat surface.

The measured forces are compared in Figure 3.2b. The gain mismatch between the two load cells is approximately 4 % which is higher than what was specified in the data-sheets. However, the estimated non-linearity is bellow 1 % for forces between 0.5 N and 5 N.

[1] XFL212R-50N from TE Connectivity. Measurement range is 50 N. Specified accuracy is 1 % of the full range

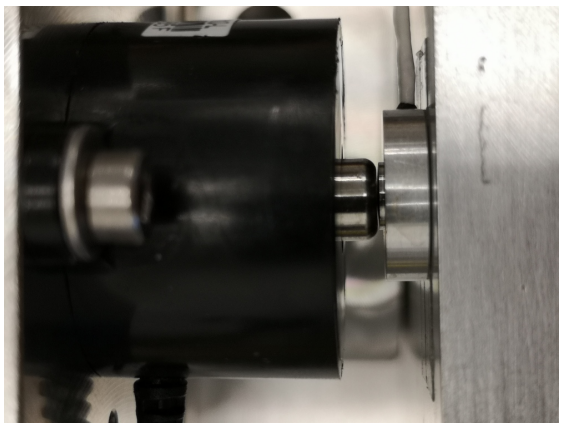

(a) Zoom on the two force sensors in contact

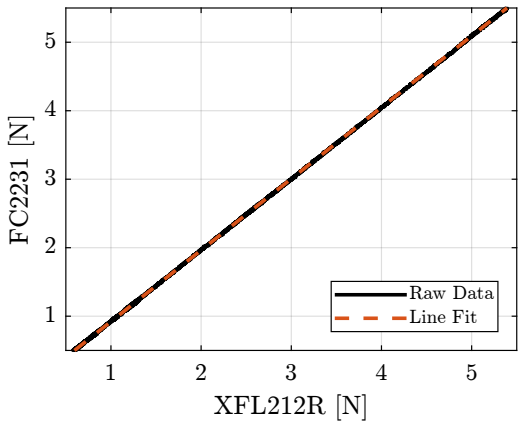

(b) Measured two force and linear fit

Figure 3.2: Caption with reference to sub figure (a), (b)

3.3 Load Cell Stiffness

The objective of this measurement is to estimate the stiffness k_F of the force sensor. To do so, a stiff element (much stiffer than the estimated $k_F \approx 1\,N/\mu m$) is fixed in front of the force sensor as shown in Figure 3.3. Then, the force sensor is pushed again this stiff element while the force and the encoder displacement are measured. Measured displacement as a function of the force is shown in Figure 3.3b. The load cell stiffness can then be estimated by computing a linear fit, and is found to be $k_F \approx 0.75\,N/\mu m$.

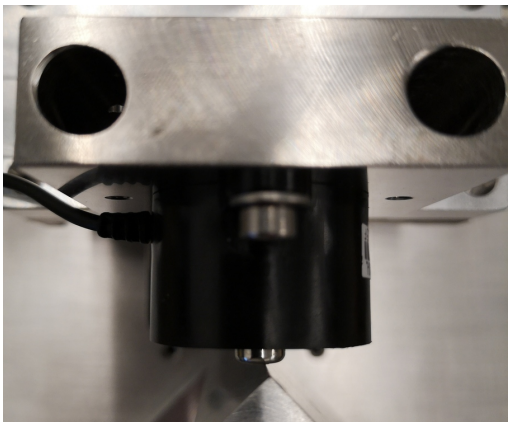

(a) Picture of the test

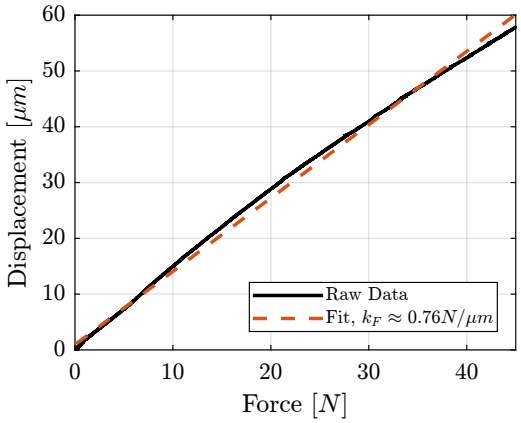

(b) Measured displacement as a function of the force

Figure 3.3: Estimation of the load cell stiffness. (a) (**??**)

3.4 Analysis of one measurement

The actual stiffness measurement in now performed by manually moving the translation stage from a start position where the force sensor is not yet in contact with the flexible joint to a position where

flexible joint is on its mechanical stop.

The measured force and displacement as a function of time are shown in Figure 3.4a. Three regions can be observed: first the force sensor tip is not in contact with the flexible joint and the measured force is zero, then the flexible joint deforms linearly, finally the flexible joint comes in contact with the mechanical stops.

The angular motion θ_y computed from the displacement d_x is displacement as function of the measured torque T_y in displayed in Figure 3.4b. The bending stiffness of the flexible joint can be estimated by computing the slope of the curve in the linear regime (red dashed line) and is found to be $k_{R_y} = 4.4\,Nm/\text{rad}$. The bending stroke can also be estimated as shown in Figure 3.4b and is found to be $\theta_{y,\max} = 20.9\,\text{mrad}$.

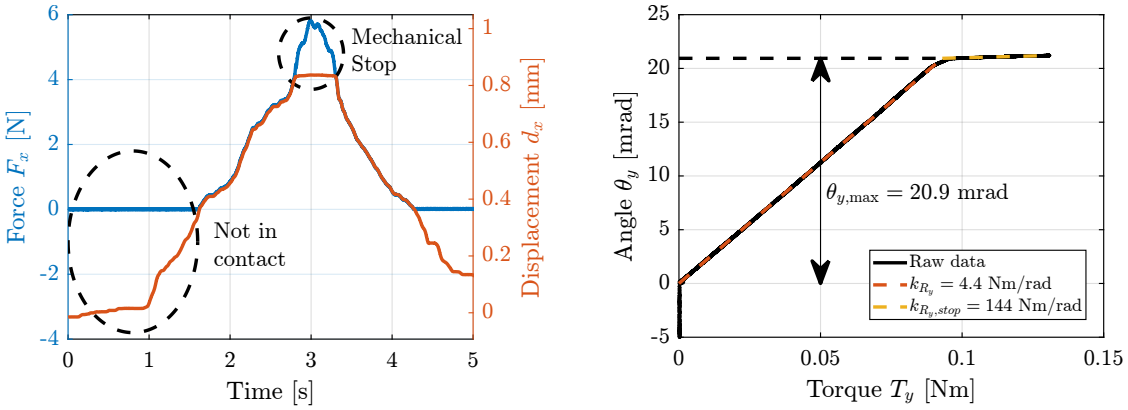

(a) Force and displacement measured as a function of time

(b) Angular displacement measured as a function of the applied torque

Figure 3.4: Results obtained on the first flexible joint. Measured force and displacement are shown in (a). The estimated angular displacement θ_y as a function of the estimated applied torque T_y is shown in (b). The bending stiffness k_{R_y} of the flexible joint can be estimated by computing a best linear fit (red dashed line).

3.5 Bending stiffness and bending stroke of all the flexible joints

Now, let's estimate the bending stiffness and stroke for all the flexible joints.

The results are summarized in Table 3.1 for the X direction and in Table 3.2 for the Y direction.

3.6 Analysis

The dispersion of the measured bending stiffness is shown in Figure 3.5 and of the bending stroke in Figure 3.6.

The relation between the measured beam thickness and the measured bending stiffness is shown in Figure 3.7.

	R_{R_x} [Nm/rad]	$k_{R_x,s}$ [Nm/rad]	$R_{x,\max}$ [mrad]
1	5.5	173.6	18.9
2	6.1	195.0	17.6
3	6.1	191.3	17.7
4	5.8	136.7	18.3
5	5.7	88.9	22.0
6	5.7	183.9	18.7
7	5.7	157.9	17.9
8	5.8	166.1	17.9
9	5.8	159.5	18.2
10	6.0	143.6	18.1
11	5.0	163.8	17.7
12	6.1	111.9	17.0
13	6.0	142.0	17.4
14	5.8	130.1	17.9
15	5.7	170.7	18.6
16	6.0	148.7	17.5

Table 3.1: Measured characteristics of the flexible joints in the X direction

	R_{R_y} [Nm/rad]	$k_{R_y,s}$ [Nm/rad]	$R_{y,\max}$ [mrad]
1	5.7	323.5	17.9
2	5.9	306.0	17.2
3	6.0	224.4	16.8
4	5.7	247.3	17.8
5	5.8	250.9	13.0
6	5.8	244.5	17.8
7	5.3	214.8	18.1
8	5.8	217.2	17.6
9	5.7	225.0	17.6
10	6.0	254.7	17.3
11	4.9	261.1	18.4
12	5.9	161.5	16.7
13	6.1	227.6	16.8
14	5.9	221.3	17.8
15	5.4	241.5	17.8
16	5.3	291.1	17.7

Table 3.2: Measured characteristics of the flexible joints in the Y direction

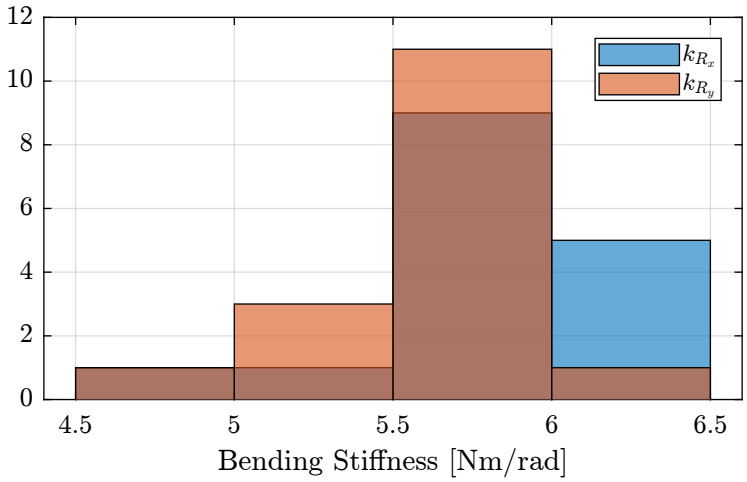

Figure 3.5: Histogram of the measured bending stiffness

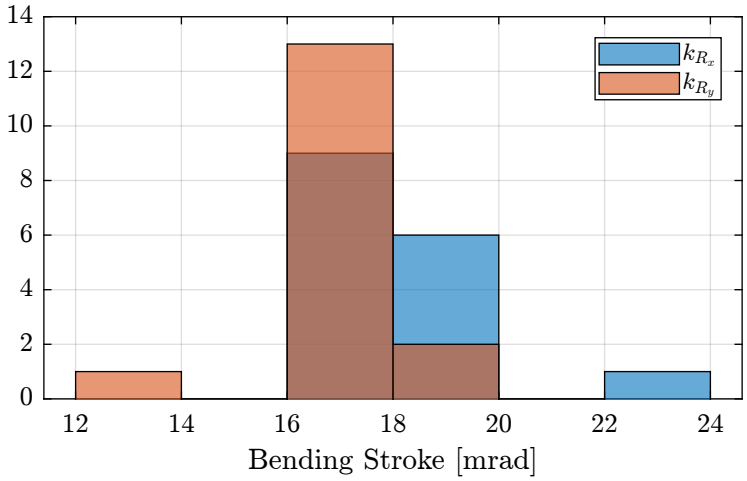

Figure 3.6: Histogram of the measured bending stroke

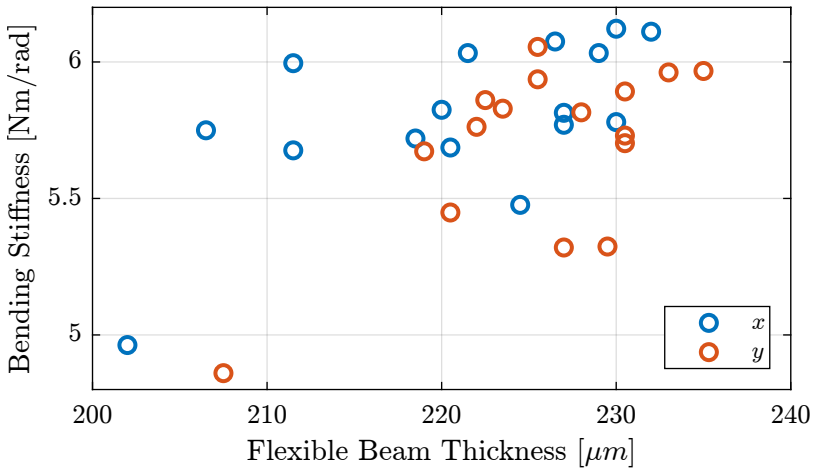

Figure 3.7: Measured bending stiffness as a function of the estimated flexible beam thickness

Conclusion

Important

The measured bending stiffness and bending stroke of the flexible joints are very close to the estimated one using a Finite Element Model.
The characteristics of all the flexible joints are also quite close to each other. This should allow us to model them with unique parameters.

4 Conclusion